NANO LETTERS

2007
Vol. 7, No. 9
2574−2577

An Improved Autonomous DNA Nanomotor

Joshua D. Bishop* and Eric Klavins

Department of Electrical Engineering, University of Washington, Seattle, Washington 98195

Received March 30, 2007; Revised Manuscript Received June 12, 2007

ABSTRACT

DNA nanomotors are synthetic biochemical devices whose motion can be controlled at the molecular scale. Some DNA devices require several exogenous additions of different types of fuel to operate, which limits their potential uses. However, several devices that operate autonomously have recently been described. One such DNA nanomotor, based on a 10−23 DNA enzyme (DNAzyme), was introduced by Chen, Wang, and Mao (*Angew. Chem., Int. Ed.* 2004, *43*, 3554). Although this DNAzyme nanomotor operates autonomously, its performance degrades over time in experiments. In this paper, we describe a mathematical model that predicts this degradation by accounting for the gradual accumulation of waste in the system. We also introduce and experimentally demonstrate two improved versions of the DNAzyme nanomotor. In particular, the new nanomotor systems use the enzyme ribonuclease H to selectively digest waste, resulting in nanomotors whose performance does not degrade significantly over time.

Nanomotors capable of controlled motion at the molecular scale have potential applications in, for example, drug delivery, gene therapy, and nanoscale manufacturing. These applications have motivated recent demonstrations of an assortment of nanomotor designs that use a variety of methods for power, control, and construction.[1−5]

Of particular interest are nanomotors made from DNA, for which several designs have been demonstrated.[6−11] This interest is due to the potential use of DNA in biological settings and to the inherent programmability and flexibility of DNA as a building block.

Most DNA nanomotors require complementary *fuel* and *anti-fuel* DNA strands to operate.[6−9] For example, a DNA nanomotor in solution can be cycled by first adding a fuel strand to open it and then adding an anti-fuel strand to close it (via strand invasion, for example[6]). The complementarity of the fuel and anti-fuel strands results in a waste product that is essentially inert but also requires that the fuel and anti-fuel strands be introduced separately.

In contrast, other DNA nanomotors do not require the separate addition of different types of fuel to operate and can therefore operate autonomously.[1,10,11] For example, the DNA nanomotor introduced by Chen, Wang, and Mao[1] is constructed from a 10−23 DNA enzyme[12] (DNAzyme), as shown in Figure 1a. This nanomotor cycles autonomously as the DNAzyme binds to fuel strands and cleaves them into *waste* strands. Unfortunately, the fuel and waste strands have similar affinities for the nanomotor. The result is that the accumulation of waste significantly interferes with the operation of the system, which can be observed experimentally as a loss of performance, as shown in Figure 1c, which represents our reproduction of the experiment by Chen, Wang, and Mao[1] (with minor modifications). This problem suggests the need to manage the waste in this system.

In this letter, we offer an explanation for the observed behavior of the DNAzyme nanomotor. This explanation suggests a modification of the DNAzyme nanomotor system, which we call the *compensated* system, that incorporates a waste management mechanism and shows improved performance in experiments. We also introduce a *streamlined* version of the compensated system that simplifies the design of the nanomotor. Both the compensated and streamlined systems use the enzyme ribonuclease H[13] (RNase H) to digest waste strands so that they do not interfere with the normal operation of the nanomotor. Finally, we offer an explanation, loosely based on the idea of disturbance rejection[14] from control theory, for the improved behavior of the compensated and streamlined systems. Specifically, we show that the original system is highly sensitive to the presence of waste, while the other systems are not.

The Original System. The DNAzyme nanomotor introduced by Chen, Wang, and Mao[1] consists of two helical arms joined by a single-base hinge on one end and an RNA-cleaving 10−23 DNAzyme on the other (see Figure 1a). The DNAzyme and a fuel strand bind to form a bulged-duplex hybrid in which conformation the nanomotor is considered open. The DNAzyme eventually cleaves the bound fuel strand and collapses, closing the nanomotor.

* Corresponding author. E-mail: jdbishop@u.washington.edu.

10.1021/nl070752s CCC: $37.00
Published on Web 07/26/2007

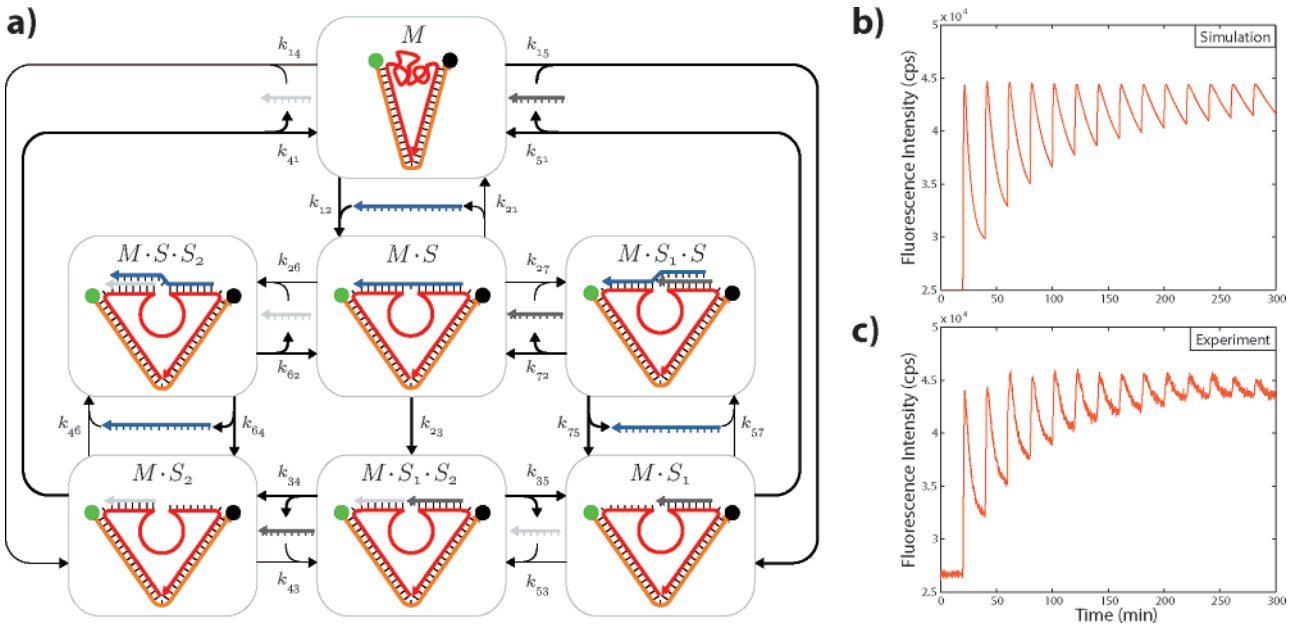

Figure 1. (a) Reaction network model of the original DNAzyme nanomotor system. The states of the nanomotor are boxed and labeled by species, where M denotes the nanomotor, S denotes the RNA fuel, and S_1 and S_2 denote the waste products. The symbol (·) denotes the hybridization of species into a larger complex. The model captures the operation of the nanomotor as well as the effect of waste having non-negligible affinity for the nanomotor. All reactions are reversible hybridization reactions, excepting the fuel-cleaving reaction, and the direction of these reactions is indicated by bold arrows. Parameters and further details are described in the Supporting Information. The model yields a simulated trajectory (b) of the system that is in agreement with our experimental results (c). In these plots, spikes in fluorescence intensity correspond to the addition of a stoichiometric quantity of RNA fuel to the solution of nanomotors.

Each nanomotor is marked with a fluorophore/quencher pair, so that the conformation of the nanomotor can be indirectly observed via fluorescence resonance energy transfer (FRET) with a spectrofluorometer. The operation of the DNAzyme nanomotor is demonstrated in a FRET experiment in which stoichiometric quantities of the RNA fuel are periodically added to a solution of the nanomotor. The experimental procedure is described in the Supporting Information.

Ideally, the RNA fuel is completely digested and the waste products are inert. In this case, the addition of fuel in a FRET experiment would be marked by a rapid rise in fluorescence intensity, followed by an exponential decline to the base fluorescence level observed before the addition. In other words, the expected behavior of the system upon continued, periodic additions of fuel is a periodic signal with constant amplitude. However, in experiments, the system does not return to the base fluorescence level after each addition of fuel, but instead saturates at a high level of fluorescence, as shown in Figure 1c, which is our reproduction of the experiment by Chen, Wang, and Mao.[1] In our experiments, we use RNA fuel strands instead of RNA/DNA chimeric strands and a different fluorophore/quencher pair, yet the results are qualitatively similar to those of Chen, Wang, and Mao.[1]

To give insight into why this behavior occurs, we describe a kinetic model of the original nanomotor system. The model includes seven species that represent all combinations of the nanomotor M bound to either the fuel S, a waste strand S_1 or S_2, or nothing on each of the binding sites of the DNAzyme. The model includes 20 reversible hybridization reactions and one irreversible cleaving reaction as shown in Figure 1a.

Using mass-action kinetics, we derive from this model a set of ordinary differential equations. We describe the details of the models and the approximation of the rate constants we use for simulation in the Supporting Information. For the simulations (in this system and the other systems we consider), we numerically solve the equations, periodically resetting the concentrations of all species to account for the periodic addition of S. An example trajectory is shown in Figure 1b, and it is in good agreement with the experimental data shown in Figure 1c.

As the experimental and simulation data show, the actual behavior of the original system is a periodic signal with decreasing amplitude. We prove in the Supporting Information that the model shown in Figure 1a predicts this behavior no matter how the values of the rate parameters are chosen. Specifically, the model suggests that an increasingly large fraction of motors remain open after each addition of fuel due to the interference of the accumulating waste strands S_1 and S_2.

The Compensated System. We infer from the model of the original system that the waste strands compete with the fuel. One way to selectively digest waste is with the enzyme RNase H, which digests RNA into triribonucleotide or smaller fragments, but only from RNA/DNA hybrids.[13] This property of RNase H ensures that the fuel is not digested before it binds to the nanomotor and that the waste products are degraded to the point of having negligible affinity for the nanomotor.

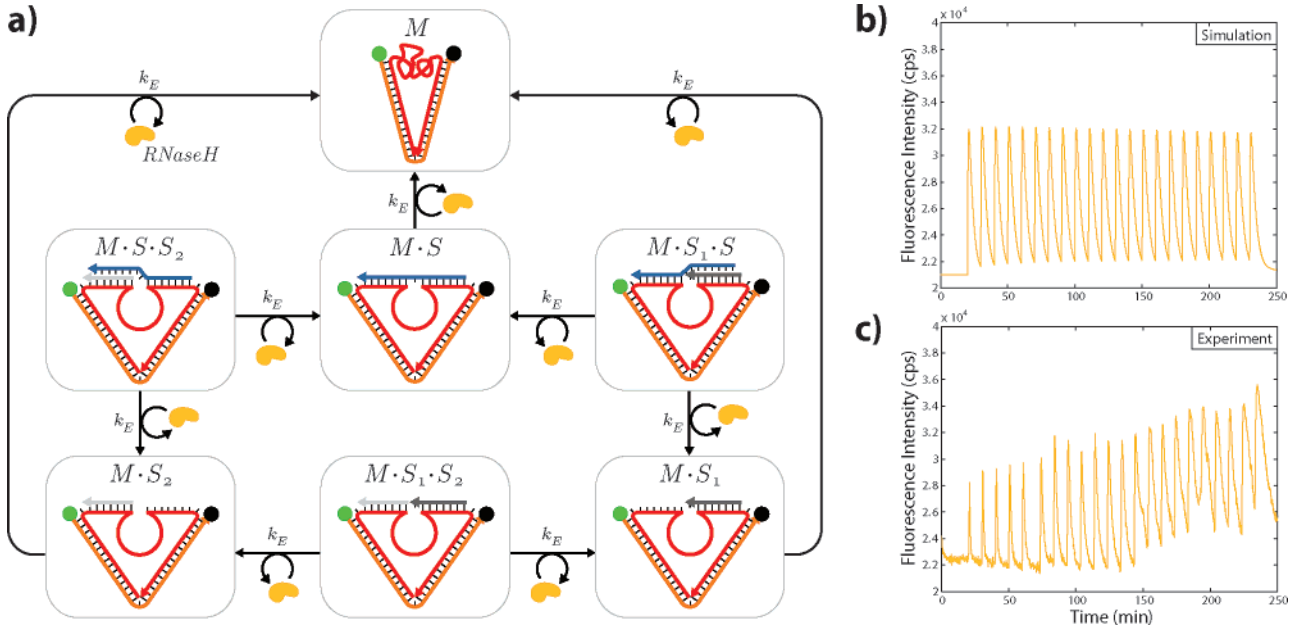

Figure 2. (a) Reaction network model of the RNase H compensator. The compensated system model is the composition of these reactions and those in the original system model depicted in Figure 1a. The enzyme RNase H degrades fuel and waste bound to motors, mitigating the effect of accumulating waste on nanomotor performance. The model yields a simulated trajectory (b) of the compensated system that is in agreement with experimental results (c). The experimental data show an upward trend not reflected in the simulated trajectory, which may be a result of nonuniform mixing or RNAase H degradation, neither of which are modeled.

The inclusion of RNase H adds reaction pathways to the original system that are shown in Figure 2a, with the estimated rate of RNA digestion by RNase H listed in the Supporting Information. We use a first-order model of enzyme kinetics for the compensated system model. These pathways mitigate the effect of the unintended pathways that dominate in the original system when the concentration of waste becomes significant. A simulation of the resulting model is shown in Figure 2b, which predicts that the performance of the compensated nanomotor system is improved over that of the original system.

Experiments confirm the behavior predicted by the modified model. Figure 2c shows experimental data for repeated additions of fuel strands to the compensated system. Further experiments (data shown in Supporting Information) show that the compensated nanomotor can be cycled even after 14 h of inactivity.

One issue is that RNase H does not distinguish between fuel bound to the nanomotor and waste bound to the nanomotor. In fact it competes with the DNAzyme to digest fuel. Thus, the two enzymes are redundant.

The Streamlined System. We introduce a streamlined design for the nanomotor in which the DNAzyme is replaced by a sequence of DNA that is exactly complementary to the RNA fuel, as shown in Figure 3a. This sequence binds with an RNA fuel strand into a full-duplex hybrid, opening the nanomotor. The RNase H then digests the bound RNA strand, closing the nanomotor. As in the compensated system, autonomy is preserved without performance loss from the accumulation of waste but with a simpler, nonredundant design.

To model the streamlined system, we consider all conformations in which RNA is bound to the nanomotor as open

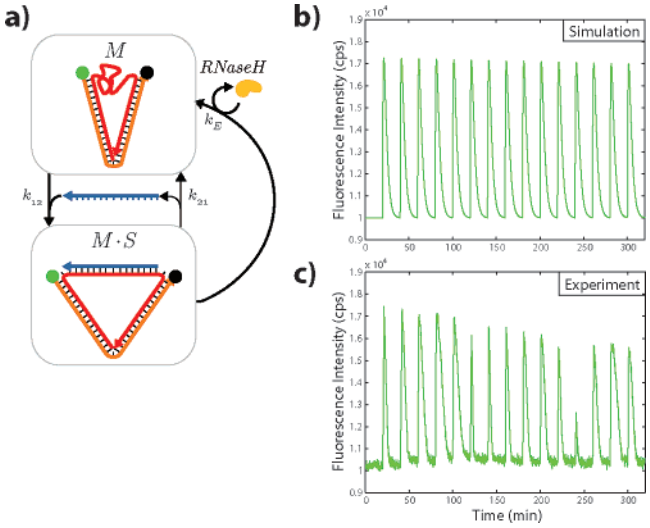

Figure 3. (a) Reaction network model of the streamlined system. The simplified nanomotor design yields a model with only two nanomotor states: *open* and *closed*. The motor opens when it binds with a fuel strand, and closes when the bound fuel is digested by RNase H. The model yields a simulated trajectory (b) of the streamlined system that is in good agreement with experimental results (c). In experiments, RNase H is replenished with every fifth addition of fuel to counteract the natural decay of the enzyme at 22 °C.

(see Figure 3a). A simulation of the resulting model is shown in Figure 3b, which predicts the same improved performance seen in the compensated system.

Experimental data from the streamlined system confirm the behavior predicted by the model. In Figure 3c, we show experimental data for repeated additions of fuel to the streamlined system. In these experiments, the activity of RNase H slowly decreases, possibly due to relatively long

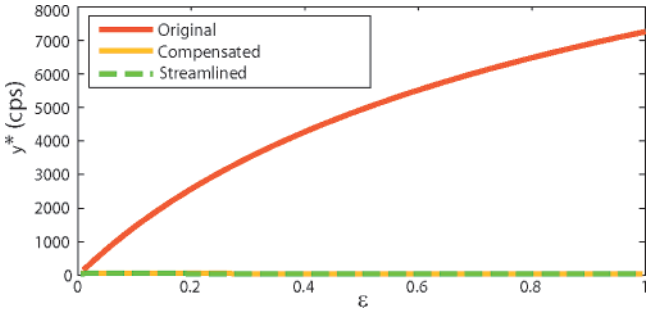

Figure 4. Plot of the sensitivity of nanomotor performance to the effect of competition from waste strands after a single addition of fuel. The performance metric, y^*, is a measure of the difference between the base fluorescence level and the equilibrium fluorescence. The dynamics for each nanomotor system are described by the equation $\dot{\mathbf{v}} = \mathbf{A}\cdot\hat{\mathbf{K}}(\mathbf{v}) + \epsilon\mathbf{A}\cdot\tilde{\mathbf{K}}(\mathbf{v})$, where $\mathbf{A}\cdot\hat{\mathbf{K}}(\mathbf{v})$ models the ideal behavior of a nanomotor system, and $\mathbf{A}\cdot\tilde{\mathbf{K}}(\mathbf{v})$ models the competition from waste strands. In the ideal case, where accumulating waste has no effect on nanomotor operation, $y^* = 0$. Although the performance of the original system is very sensitive to competition from waste strands, the performance of the compensated and streamlined systems is completely insensitive to this competition.

exposure to room temperature. Thus, we replenish the RNase H with every fifth addition of fuel to the system.

Discussion. Biochemical nanodevices have been demonstrated in simple laboratory settings. However, to be useful, nanodevices must eventually be deployed in more complex settings and in the presence of other devices. Thus, a truly useful nanodevice must be robust to its operating environment. It is instructive to characterize the present work in the context of robustness.

For example, given a model of the ideal behavior of the DNAzyme nanomotor, we characterize the effect of increasing concentrations of waste products as a *disturbance*. In particular, we write the dynamics as

$$\dot{\mathbf{v}} = \mathbf{A}\cdot\hat{\mathbf{K}}(\mathbf{v}) + \epsilon\mathbf{A}\cdot\tilde{\mathbf{K}}(\mathbf{v})$$

Here, the stoichiometric matric $\mathbf{A}$ with the rate function $\hat{\mathbf{K}}$ models the ideal behavior (with no competition from the waste strands), and $\mathbf{A}$ with $\tilde{\mathbf{K}}$ models the disturbance (in which competition is present). We use the equilibrium fluorescence intensity y^* as a performance metric. Details of the sensitivity analysis for each system are included in the Supporting Information. In Figure 4, we show the *sensitivity* of y^* to ϵ after the addition of a stoichiometric quantity of fuel for all three of the systems described in this paper. The original system is highly sensitive to the disturbance, as is evident from the dependence of y^* on ϵ. In contrast, the compensated and streamlined systems are completely insensitive to the disturbance, indicating that these systems are robust to competition from waste strands.

It appears that a biochemical nanodevice, even a very simple nanomotor, requires a control system to regulate its performance and increase its robustness. For example, the pathways resulting from the inclusion of RNase H to the DNAzyme nanomotor system can be considered to be a rudimentary control system. We speculate that more complex, integrated, and interconnected nanodevices will require equally complex control systems that govern their behaviors.

Acknowledgment. We thank Erik Winfree and Niles Pierce (California Institute of Technology) and Fayette Shaw (University of Washington). This work was partially supported by the University of Washington Royalty Research Fund.

Supporting Information Available: DNA and RNA sequences, nanomotor formation, FRET analysis, model and simulation details, parameter estimation, and details of the sensitivity analysis. This material is available free of charge via the Internet at http://pubs.acs.org.

References

(1) Chen, Y.; Wang, M.; Mao, C. *Angew. Chem., Int. Ed.* **2004**, *43*, 3554.
(2) Koumura, N.; Zijlstra, R. W.; van Delden, R. A.; Harada, N.; Feringa, B. L. *Nature* **1999**, *401*, 152.
(3) Fennimore, A. M.; Yuzvinsky, T. D.; Han, W. Q.; Fuhrer, M. S.; Cumings, J. *Nature* **2003**, *424*, 408.
(4) Regan, B. C.; Aloni, S.; Jensen, K.; Zettl, A. *Appl. Phy. Lett.* **2005**, *86*, 123119.
(5) Balzani, V.; Clemente-Leon, M.; Credi, A.; Ferrer, B.; Venturi, M.; Flood, A. H.; Stoddart, J. F. *Proc. Natl. Acad. Sci. U.S.A.* **2006**, *103*, 1178.
(6) Yurke, B.; Turberfield, A. J.; Mills, A. P., Jr.; Simmel, F. C.; Neumann, J. L. *Nature* **2000**, *406*, 605.
(7) Shin, J. S.; Pierce, N. A. *J. Am. Chem. Soc.* **2004**, *126*, 10834.
(8) Tian, Y.; Mao, C. *J. Am. Chem. Soc.* **2004**, *126*, 11410.
(9) Li, J. J.; Tan, W. *Nano Lett.* **2002**, *2*, 315.
(10) Turberfield, A. J.; Mitchell, J. C.; Yurke, B.; Mills, A. P., Jr.; Blakey, M. I.; Simmel, F. C. *Phys. Rev. Lett.* **2003**, *90*, 118102.
(11) Yin, P.; Yan, H.; Daniell, X. G.; Turberfield, A. J.; Reif, J. H. *Angew. Chem., Int. Ed.* **2004**, *43*, 4906.
(12) Santoro, S. W.; Joyce, G. F. *Proc. Natl. Acad. Sci. U.S.A.* **1997**, *94*, 4262.
(13) Miller, H. I.; Gill, G. N.; Riggs, A. D. *J. Biol. Chem.* **1973**, *248*, 2621.
(14) Doyle, J. C.; Francis, B. A.; Tannenbaum, A. R. *Feedback Control Theory*; MacMillan: New York, 1992; Chapter 1.

NL070752S